

Chapter 17

Development and Applications of ARM Millimeter-Wavelength Cloud Radars

PAVLOS KOLLIAS,^{a,k} EUGENE E. CLOTHIAUX,^b THOMAS P. ACKERMAN,^c BRUCE A. ALBRECHT,^d
KEVIN B. WIDENER,^e KEN P. MORAN,^f EDWARD P. LUKE,^g KAREN L. JOHNSON,^g NITIN BHARADWAJ,^e
JAMES B. MEAD,^h MARK A. MILLER,ⁱ JOHANNES VERLINDE,^b ROGER T. MARCHAND,^c
AND GERALD G. MACE^j

^a McGill University, Montreal, Quebec, Canada

^b The Pennsylvania State University, University Park, Pennsylvania

^c University of Washington, Seattle, Washington

^d University of Miami, Miami, Florida

^e Pacific Northwest National Laboratory, Richland, Washington

^f National Oceanic and Atmospheric Administration, Boulder, Colorado

^g Brookhaven National Laboratory, Upton, New York

^h ProSensing, Inc., Amherst, Massachusetts

ⁱ Rutgers, The State University of New Jersey, New Brunswick, New Jersey

^j University of Utah, Salt Lake City, Utah

1. Introduction

As the ARM Program was getting underway in the early 1990s, studies by [Ramanathan et al. \(1989\)](#) and [Cess et al. \(1990\)](#) highlighted the importance of cloud and radiation interactions to climate. [Ramanathan et al. \(1989\)](#) demonstrated that, on average, clouds cool the climate system but that different cloud types can have different influences upon it. [Cess et al. \(1990\)](#) showed that general circulation models have an array of different responses to the same sea surface temperature change that result from differences in model clouds and their interactions with radiation. In their papers discussing the ARM Program, [Stokes and Schwartz \(1994\)](#) and later [Ackerman and Stokes \(2003\)](#) emphasized the importance of characterizing clouds throughout a vertical column in order to fully understand the radiation field associated with them. They

made clear that coupling of high-fidelity observations of clouds and radiation were necessary to improving model parameterizations of them, which were in turn necessary for improving prognostic models of future climate.

Lidar and radar are two key technologies for remote sensing of cloud properties through vertical columns of the atmosphere. Lidar remote sensing of cirrus cloud properties was already a well-developed discipline in the early 1990s (e.g., [Sassen et al. 1990](#)) with a focus on understanding cirrus microphysical and radiative properties and their importance to climate (e.g., [Platt et al. 1987](#)). [Stokes and Schwartz \(1994\)](#) recognized the importance of lidar to the ARM Program; in fact, many of the coauthors of the [Sassen et al. \(1990\)](#) and [Platt et al. \(1987\)](#) papers, as well as their institutional colleagues, were listed by [Stokes and Schwartz \(1994\)](#) as early investigators in the ARM Program.

While lidar is the optimal instrument for studying optically (in the visible and infrared regions of the electromagnetic spectrum) thin clouds, this technology is limited for study of optically thick clouds, which attenuate the lidar beams. Optically thick clouds are often transparent at the longer microwave wavelengths, so the importance of microwave radar remote sensing of clouds was also clear at this time. As the ARM Program started, radar remote sensing of cloud properties in support of climate studies was not nearly as mature as that for lidar. The development of millimeter-wavelength radar technology and its conversion

^k Current affiliation: School of Marine and Atmospheric Sciences, Stony Brook University, State University of New York, Stony Brook, New York.

Corresponding author address: Pavlos Kollias, Institute of Terrestrial and Planetary Atmospheres, School of Marine and Atmospheric Sciences, Stony Brook University, State University of New York, Stony Brook, NY 11794-5000.
E-mail: pavlos.kollias@stonybrook.edu

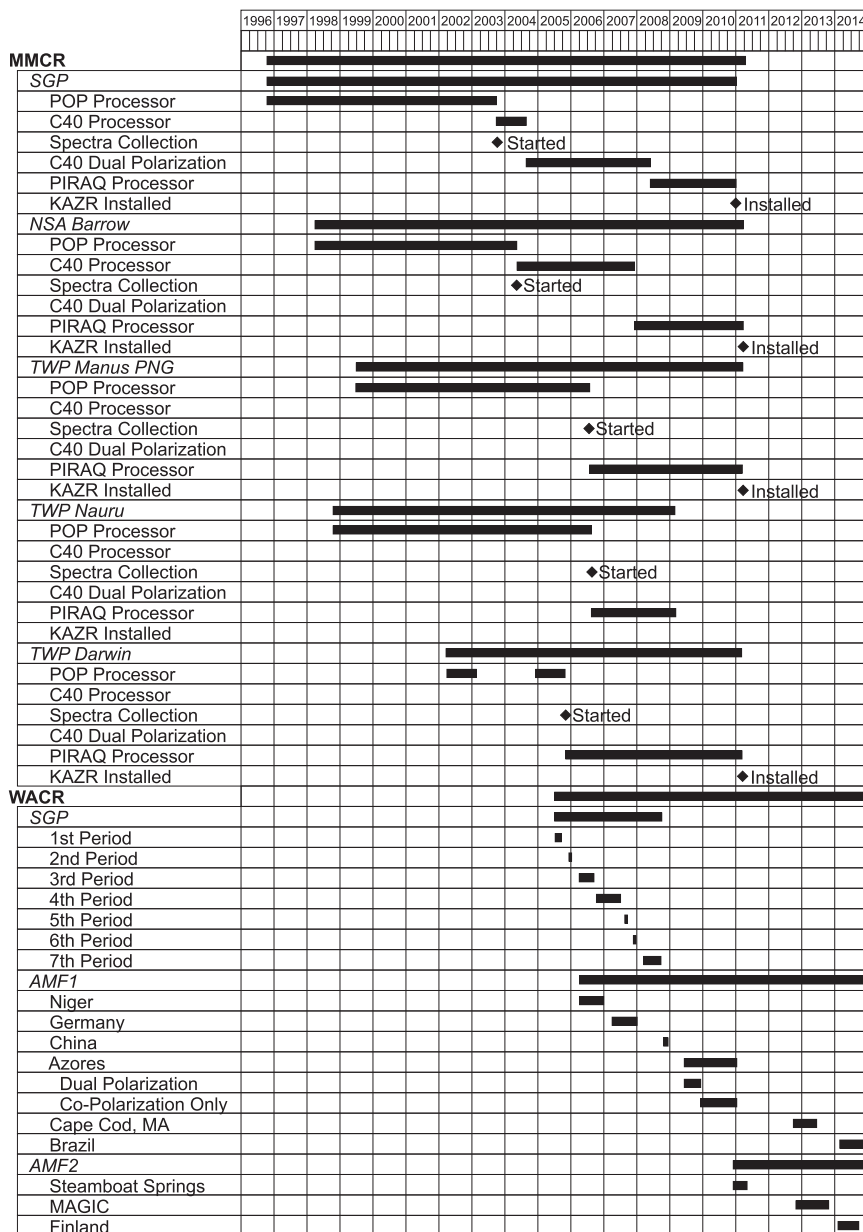


FIG. 17-1. Timeline of the key developments in the 20-yr history of the ARM cloud radar.

to an automated, operational system is a notable achievement of the ARM Program.

When the ARM Program began, the only millimeter-wavelength radars available for meteorological research deployment were a 35-GHz system managed by the National Oceanic and Atmospheric Administration (NOAA) Wave Propagation Laboratory and a 94-GHz system developed by Roger Lhermitte at the University of Miami. In addition, the Pennsylvania State University research group headed by Bruce Albrecht was in the process of building a deployable system funded by the Office of Naval Research.

Now, 20 years later, the ARM Program supports a suite of millimeter-wavelength radars at each of its permanent sites and mobile facilities (Fig. 17-1). The data from these radars have, in many ways, revolutionized our knowledge of cloud structure and cloud processes, and we expect that new data will continue to expand our understanding in these areas (e.g., Kollias et al. 2007a). The success of the ARM Program has fostered the development and deployment of additional millimeter-wavelength radars at several sites in Europe and Asia. The proposal that ultimately led to the launch of the National Aeronautics and Space Administration (NASA)

TABLE 17-1. Various types of radars used in the atmospheric sciences today.

Designation	Band	Frequency (GHz)	Wavelength (mm)
Cloud mm-wave	W	75.0–110.0 (WACR: 95.04; W-SACR: 93.93)	2.7–4.0 (WACR: 3.15; W-SACR: 3.19)
Cloud mm-wave	Ka	26.5–40.0 (MMCR/KAZR: 34.86; Ka-SACR: 35.29)	7.5–11.3 (MMCR/KAZR: 8.6; Ka-SACR: 8.5)
Cloud/precipitation mm-wave	Ku	12.0–18.0	16.7–25.0
Cloud/precipitation cm-wave	X	8.0–12.0 (X-SACR: 9.73)	25.0–37.5 (X-SACR: 30.8)
Cloud/precipitation cm-wave	C	4.0–8.0	37.5–75.0
Weather cm-wave	S	2.0–4.0 (NOAA 3-GHz profiler: 2.835)	75.0–150.0 (NOAA 3-GHz profiler: 106)

CloudSat radar relied heavily on results obtained by the ARM Program. The goal of this chapter is to describe the evolution and current status of the ARM Program millimeter-wavelength radar effort.

2. A brief primer on cloud radar terminology and parameters

As the operating wavelength of radar becomes longer, its capability to detect small particles (e.g., cloud drops or ice crystals) decreases. This decrease is because the scattering efficiency is inversely proportional to wavelength to the fourth power for small particles. This loss in scattering efficiency with increasing wavelength can be offset to an extent by increased transmitter power and antenna size at the longer wavelengths. Furthermore, attenuation due to liquid water increases roughly as frequency squared. Taking into consideration all of these effects, practical ground-based cloud radar systems operating at Ka band have the highest sensitivity, followed by W band. In contrast, weather radars, which are used to track precipitation, utilize long wavelengths because their beams must penetrate to far distances and their targets of interest are large, precipitating particles. Table 17-1 illustrates the range of centimeter- and millimeter-wavelength radars commonly used in the atmospheric sciences today, together with ways of identifying them.

Millimeter-wavelength cloud radars (MMCRs) specific to the ARM Program are listed in Table 17-2. The ARM radars use shorter wavelengths in order to enhance their sensitivity to small cloud drops and ice crystals. However, as Table 17-2 illustrates, there are many other features of the ARM radars that are relevant to their sensitivity. For example, as the antenna diameter of a radar increases, so does its sensitivity; as the length of the pulses that it transmits increases, so does the power that it is sending up into the atmosphere, leading to enhanced sensitivity. Similarly, if the pulse repetition frequency (PRF) increases, more pulses are transmitted into the atmosphere per unit time, leading to an enhancement of radar sensitivity through signal integration. While transmitting longer

pulses into the atmosphere increases sensitivity, doing so leads to a degradation of spatial resolution along the beam. To circumvent this trade-off, pulse compression, or pulse coding, techniques are implemented on some ARM radars. These techniques are ones for which the radar transmits long pulses, but with modulations within them to encode extra information, to enhance sensitivity but in which additional signal processing techniques that utilize the encoded information in the pulses are applied to the returned powers to maintain high spatial resolution.

Each pulse transmitted by radar leads to continuous (in time) power scattered back to the radar by the atmospheric constituents encountered by the radar pulse. In this case, time is equivalent to range (or distance) from the radar, and each sample of this return power by the radar receiver leads to an output signal corresponding to a particular range, or range gate, from the radar. A time series of output signals corresponding to different distances from the radar results from a single pulse, and multiple pulses lead to multiple time series of these range-dependent output signals. Radars are designed to analyze the output signals from multiple pulses that correspond to the same range gate (i.e., the same distance from the radar). These signals originating from the same range gate, called in-phase/quadrature-phase (I/Q) data, can be analyzed via fast Fourier transforms (FFTs) to produce spectra from which power (the zero-Doppler moment), mean Doppler velocity (the first Doppler moment), and Doppler spectral width (the second Doppler moment) estimates of the cloud particles at this range can be inferred.

A technique called coherent integration was used by ARM in the earlier days, in which up to 10 successive I/Q samples at a particular range gate were summed prior to FFT processing to improve signal-to-noise ratio. Although coherent integration is computationally efficient, the signal-to-noise improvement rolls off with increasing Doppler shift. Later signal processors in the W-Band ARM Cloud Radar (WACR) and Ka-Band ARM Zenith-Pointing Radar (KAZR) achieved the same overall processing gain without Doppler velocity-dependent errors by increasing the length of the FFT.

TABLE 17-2. Specifications of ARM Program profiling cloud radars. NLFM—nonlinear frequency modulation.

Parameter	MMCR (1995–2004)	MMCR (2004–10)	WACR (2005–present)	KAZR (2011–present)
Transmitter type	TWTA	TWTA	EIKA	TWTA
Frequency (GHz)	34.86	34.86	95.00	34.86
Pulse compression	Barker	Barker	No	NLFM
Pulse length (ns)	300–19 200	300–19 200	300	300–12 000
Antenna size (m)	2.0 (3.0) ^a	2.0 (3.0) ^a	1.8	2.0 (3.0) ^a
3-dB beamwidth	0.31 (0.19) ^a	0.31 (0.19) ^a	0.19	0.31 (0.19) ^a
PRF range (kHz)	6.0–14.0	6.0–14.0	7.5–10.0	3.0–10.0
Tx polarization	Linear	Linear	Linear	Linear
Rx polarization	Copolar	Co/cross-polar	Co/cross-polar	Co/cross-polar
Saturation (dBZe) at 1 km	+20	+20	+10	+35
Coherent integration	Yes	Yes	No	No
Signal dwell (sec)	9	2	2	2
Number of operational modes	4 (BL, CI, GE, PR)	5 (BL, CI, GE, PR, PO)	2 (GE, PO)	2 (GE, PO)
Mode sequence period (sec)	36	12–14	4	2
Receiver efficiency (%)	3–25	60–70	100	100
FFT length	64	128–256	256	256
Spectra recording	No	Yes	Yes	Yes

^a At the SGP site.

Although several combinations of radar parameters can be selected, as discussed above, each comes with strengths and weaknesses. Specific combinations of radar parameters implemented for the ARM radars are called modes, and the more modes that the radar cycles through, the longer it takes before a mode is revisited. Table 17-2 illustrates that, as the ARM Program has progressed, the capability of the ARM radars has improved so that fewer modes need to be run to accomplish specific scientific objectives. Moreover, the efficiency (i.e., the percentage of pulses that the radar transmits that are processed by the data system—a measure of the data system’s ability to keep up with the radar transmitter) of the ARM radars has improved, finally reaching 100%. This increase in efficiency has led to smaller time periods, called dwell times, necessary for the radar to collect and process the same number of pulses, leading to significant improvements in temporal resolution without a loss of sensitivity.

One final notable feature evident in Table 17-2 is the gradual implementation of polarization diversity on the ARM radars. The first ARM radars transmitted (Tx) linearly polarized electromagnetic radiation and received (Rx) only the copolarized signal (i.e., the signal that has the same polarization as the transmitted wave). In 2004, the ARM radars were upgraded to receive both the copolarized and cross-polarized signals.

3. The beginnings of the DOE ARM Program cloud radar

The first cloud radar, the MMCR, developed by the ARM Program was deployed at the ARM Southern

Great Plains (SGP) site in 1996. A search through the ARM data archive yields the date of 8 November 1996 for the first file generated by this MMCR. Many technical achievements over the decades after World War II enabled the generation of this first file. So what are the watershed events that led to the development of the ARM Program’s cloud radar activities? From our perspective, these events were the First ISCCP Regional Experiments (FIRE) Second Cirrus Intensive Field Observation (IFO) campaign in southern Kansas from 13 November 1991 through 7 December 1991 (e.g., Uttal et al. 1995) and the FIRE Second Marine Stratocumulus IFO campaign in the Azores Islands in the eastern North Atlantic from 1 June 1992 through 28 June 1992 (Albrecht et al. 1995).

The FIRE Second Cirrus IFO campaign in Kansas was the prototype for the ARM SGP site (Sisterson et al. 2016, chapter 6). Although it was only a month-long field campaign, the FIRE experiment brought together for the first time at a single site many instruments, each with a separate heritage and representing state-of-the-art remote sensing of cloud properties, to make measurements in the same or adjacent volumes of atmospheric air in support of cloud and radiation studies. These instruments included the dual-polarimetric, scanning Ka-band (35 GHz) Doppler radar developed by NOAA (e.g., Pasqualucci et al. 1983), the W-band (94 GHz) Doppler radar developed by the Pennsylvania State University (Clothiaux et al. 1995) using the design of Lhermitte (1987), and a suite of four lidars (e.g., Sassen et al. 1995). The FIRE Second Cirrus IFO in Kansas was collocated and coincident with the DOE- and NASA-funded Spectral Radiance Experiment (SPECTRE),

which collected state-of-the-art surface radiation measurements (Ellingson and Wiscombe 1996; Ellingson et al. 2016, chapter 1). One of the key outcomes of the FIRE Second Cirrus IFO campaign was that the Pennsylvania State University W-band radar was run quasi operationally for the entire IFO period. The FIRE Second Marine Stratocumulus IFO campaign that followed six months later provided additional support for the use of millimeter-wavelength radar by demonstrating that the radar could be transported easily to a somewhat remote location and used again in a quasi-operational mode in conjunction with other instruments, including the NOAA Ka-band radar, to investigate cloud properties. Equally importantly, the Pennsylvania State University and NOAA groups, among others, demonstrated the scientific utility of the radar data and began the development of analysis software for the radar, including an early version of a cloud mask algorithm (e.g., Clothiaux et al. 1995; Miller and Albrecht 1995; Uttal et al. 1995; Danne et al. 1996).

These two field campaigns, particularly the FIRE Second Cirrus IFO campaign in conjunction with SPECTRE, represented the early beginnings of the ARM Program's radar activities that focused on clouds and radiation measurements in support of understanding cloud processes and improving climate models (Stokes 2016, chapter 2). With ARM sites envisioned in remote areas of the world, ARM's cloud radar faced numerous challenges beyond those early field campaigns, including going beyond quasi-continuous operation of cloud radars to full 24/7 operations with no onsite technical support.

4. The need for enhanced radar sensitivity

Measurements from the FIRE Second Cirrus IFO campaign made one thing abundantly clear. Although MMCRs could detect many types of clouds, they were not able to match the sensitivity of the lidars in detecting thin cirrus. Inspection of the displays of the polarization diversity lidar during cirrus case study periods showed that, at times, the upper troposphere contained an abundance of ice crystals that were below the detection limit of the Ka- and W-band radars. In the case of thicker cirrus, the radar and lidar observations of cirrus extent often coincided. These early observations during the FIRE Second Cirrus IFO campaign established the necessity of building cloud radars for the ARM Program with as much sensitivity as technically possible.

5. Mitigating the impacts of attenuation at cloud radar operating frequencies

During the FIRE Second Marine Stratocumulus IFO campaign in the Azores Islands, high-powered lidars

were not available. The cloud radars, low-powered laser ceilometers, and passive microwave radiometers were the tools of the day. The reasons for the change from the FIRE Second Cirrus IFO campaign were obvious: the marine clouds that shrouded the Azores Islands during the campaign were thick liquid water clouds, the numerous droplets of which rapidly attenuated lidar signals, making these clouds of less interest to the lidar community. These clouds were detected readily by the cloud radars, which consistently profiled the location of cloud liquid water from cloud base to cloud top (Frisch et al. 1995; Miller and Albrecht 1995). In the marine boundary layer during this campaign, as well as for the FIRE Second Cirrus IFO campaign, attenuation of the cloud radar signals was not a dominant issue. In the case of water vapor and liquid water attenuation, Ka-band cloud radars have a clear advantage over W-band radars because absorption is significantly less at the longer wavelength; W-band attenuation is often severe in rain or clouds of high liquid water content or when scanning horizontally through regions of high humidity.

Nowhere was the attenuation difference better demonstrated than during the Maritime Continent Thunderstorm Experiment (MCTEX; Keenan et al. 2000) in the Tiwi Islands, Northern Territory, Australia, November and December 1995. These islands are famous for Hector, which are massive thunderstorms that develop over them every early afternoon at this time of the year. For the MCTEX experiment, the University of Massachusetts deployed a dual-frequency Ka/W-Band cloud profiling radar system (CPRS; Mead et al. 1994), while NOAA deployed a vertically pointing S-band radar (Ecklund et al. 1999). On one occasion, a Hector formed right over the radar installation; at this time, the W-band radar signal completely attenuated by 200 m and the Ka-band by 2 km, but the S-band radar detected hydrometeors up to 18 km of altitude. These observations indicate that, while shorter-wavelength radars are better able to detect small hydrometeors, longer-wavelength radars have value in detecting larger hydrometeors in cases where attenuation of the shorter-wavelength radar beams is severe.

6. The ARM Program MMCRs

One of the early discussions in the ARM Program was whether to deploy Ka- or W-band radars to its sites. W-band radar signals have greater sensitivity to small hydrometeors, while Ka-band radar signals suffer less attenuation. The decision was made to go with Ka-band radar for several reasons of roughly equal weight. First, Ka-band wavelengths suffer less attenuation. Second, Ka-band technology was considered more robust than W-band technology because the radar community had

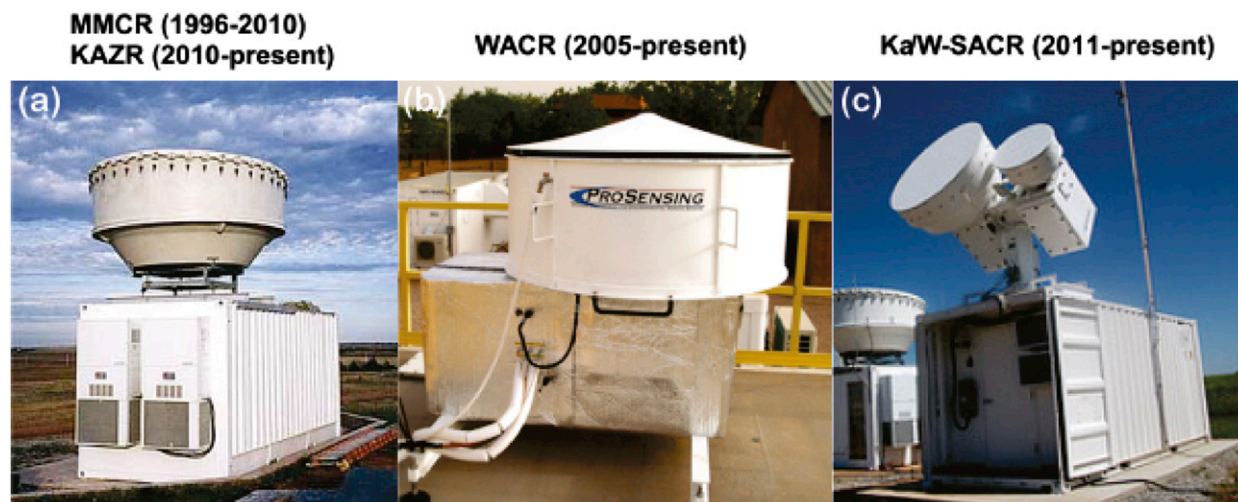


FIG. 17-2. (a) The MMCR with its 10-ft antenna at the ARM SGP site; the KAZR has a similar external design to the MMCR; (b) the WACR; and (c) the Ka/W-SACR.

more experience with it. (As it turned out, W-band components were equally robust, but that was unclear at the time.) Third, W-band components were more expensive than Ka-band components.¹

The NOAA radar group was quite familiar with Ka-band radar technology and was selected to develop a Ka-band cloud radar system to be deployed at each of the ARM fixed sites. The first system was deployed at the SGP site in 1996 (Fig. 17-2a). The design focus was on enhancing radar sensitivity. Moran et al.'s (1998) paper on the design of the ARM MMCR emphasized the importance of sensitivity and design features that were intended to enhance it, primarily the pulse-coded radar signals that delivered both sensitivity and high spatial resolution (Figs. 17-3a,b). Because the pulse-coded waveforms had detrimental effects close to the surface, especially evident in Fig. 17-3a, Moran et al. (1998) designed several different operational modes for the radar (Figs. 17-3a-d), each one intended for detection of specific cloud types. The coded long-pulse "cirrus" mode (Fig. 17-3a) was designed for maximum sensitivity but with contamination issues close to the surface. The coded short-pulse "boundary layer" mode (Fig. 17-3b) was designed for as much sensitivity as possible to thin boundary layer clouds while minimizing clutter near the surface. The "general" mode (Fig. 17-3c) was designed to be an artifact-free mode but with

saturation issues during precipitation (see Table 17-2 for the reflectivities at 1 km that lead to saturation, or too much power for the receiver to handle linearly). The "precipitation" mode was designed as a robust mode that minimized all known artifacts (e.g., velocity folding) but unfortunately did not address receiver saturation. Sensitivity of all modes was also enhanced by the use of a large antenna with a 10-ft diameter at the SGP site. Smaller, 6-ft-diameter antennas were used at the remote sites because the large 10-ft antenna could not fit into the sea containers used for transportation.

Another innovation sought from the beginning of the ARM Program was collection of spectral data in addition to moments. Unfortunately, the data volumes associated with spectral data were too high to transmit routinely over the Internet when the ARM Program got underway. This was true of the ARM SGP site where communications were best, as well as for the remote ARM Tropical Western Pacific (TWP) and North Slope of Alaska (NSA) sites, where communications were much more severely limited. The ARM Program has worked continuously to improve data handling and with much success, as will become clear later.

7. Identifying weak returns and dealing with atmospheric plankton

Associated with specialized hardware for maximizing radar sensitivity came the need for processing software that built upon it. No longer was it sufficient to apply a simple threshold to radar return signals in identification of hydrometeors, as is often done with lower-frequency precipitation radars, where signal-to-noise ratio is typically high. Cloud radar signals, especially for thin clouds,

¹ At an early ARM Program science team meeting, the ARM Chief Scientist Gerald Stokes sent Thomas Ackerman, Robert Kropfli, and Robert McIntosh off to a corner and told them to come back with a final recommendation for the millimeter-wavelength system. Their consensus was a Ka-band radar.

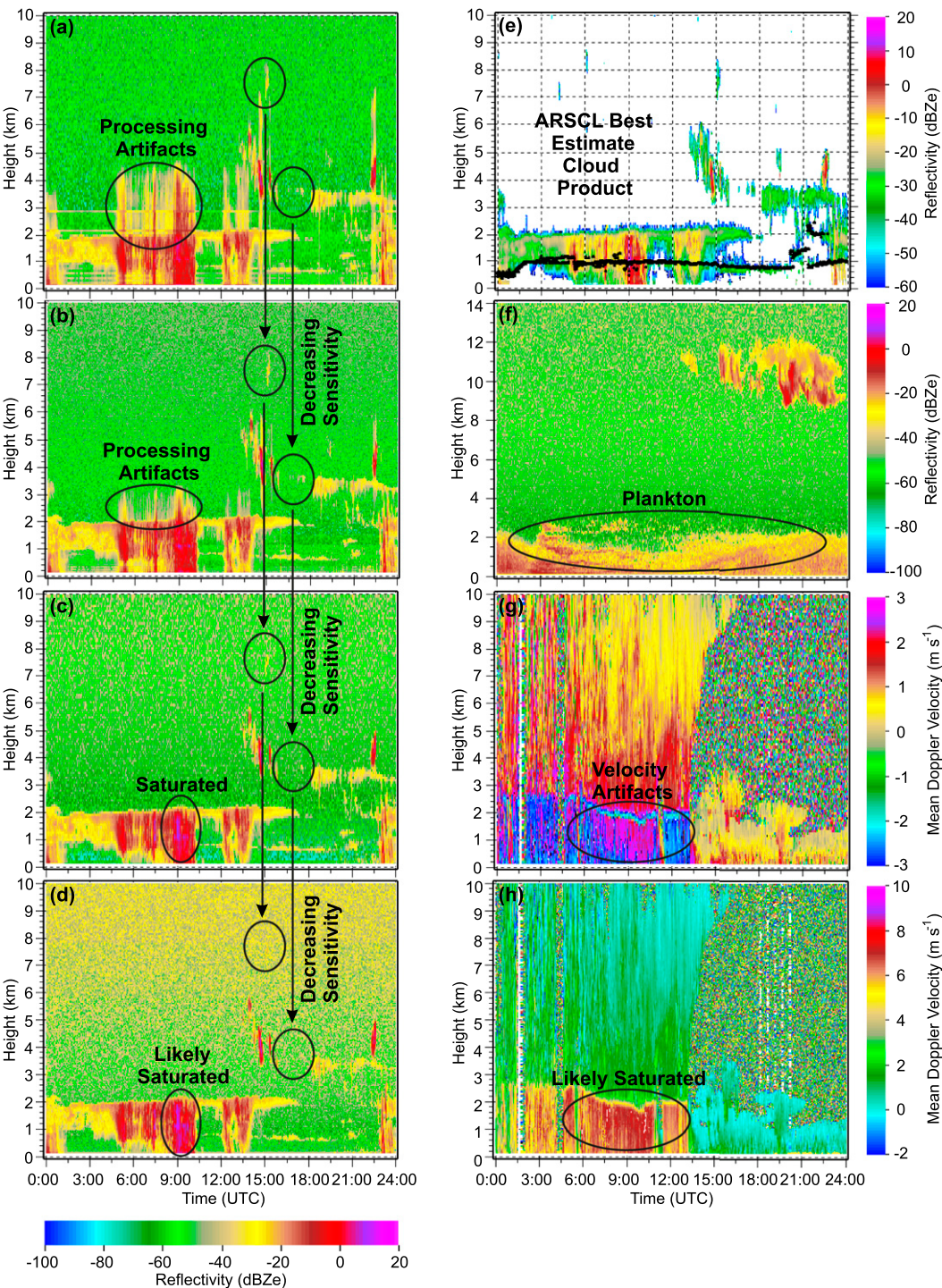


FIG. 17-3. MCCR mode data on 9 Apr 1997 for the (a) coded long-pulse cirrus (CI) mode, (b) coded short-pulse boundary layer (BL) mode, (c) general mode, and (d) precipitation (PR) mode. (e) The ARSCL VAP for 9 Apr 1997. (f) Particularly severe atmospheric plankton in the general mode on 19 Jun 1997. Mean Doppler velocities on 11 Apr 1997 for the (g) general and (h) precipitation modes.

are often buried in the noise, and effort is required to isolate signal from noise. Clothiaux et al. (1995) investigated two different spatial filters for extracting signals from noise, and Clothiaux et al. (2000) implemented spatial filtering in the operational processing of MMCR Doppler moments. The output of the signal extraction, mode merging, and plankton clearing processing came to be called the Active Remote Sensing of Clouds (ARSCL) value-added product (VAP; Fig. 17-3e). As they pointed out, the two most important elements of operational processing of MMCR data are extracting weak signals from the noise and distinguishing signals from insects, spider webs, floating agricultural debris, and any other nonhydrometeor return, or what came to be called “atmospheric plankton” after Lhermitte (1966).

The complicating effects of atmospheric plankton should not be underestimated, especially during the warm months at the ARM sites. Many of the examples of MMCR signal returns in Moran et al. (1998) were from relatively warm months—12 May 1997 (their Fig. 3), 10 April 1997 (their Fig. 4), and 19 June 1997 (their Fig. 5)—and these examples clearly demonstrate strong radar signals from atmospheric plankton below approximately 2 km of altitude, where it often dominates the signals. A worst-case example occurred on 19 June 1997 (their Fig. 5 and reproduced here as Fig. 17-3f) when the atmospheric plankton dominated the signal up to 2.5 km of altitude and could be seen sporadically as high as 3 km of altitude. These returns from non-meteorological targets severely complicate the operational processing of MMCR signals to isolate the cloud and precipitation returns. A procedure was developed for operational processing of MMCR data using lidar signal returns, which were unaffected by atmospheric plankton, to aid in identifying returns from hydrometeors and atmospheric plankton. However, this approach was not optimal, only allowing for the identification of plankton below cloud base.

The following techniques have been used with some success to identify plankton:

- Examination of linear depolarization ratio (LDR; i.e., the ratio of the power received in the orthogonal, or cross-polarized, channel to that received in the transmission, or copolarized, channel of a dual-receiver channel radar when a linearly polarized signal is transmitted);
- Processing of high-frequency (pulse-by-pulse) radar returns (i.e., the I/Q data);
- Examination of the shape of the radar Doppler spectra (Luke et al. 2008).

Nonetheless, the effect of plankton is much smaller at W band, which has been one of the factors prompting

the ARM Program to deploy W-band radars in recent years.

The significant contributions of atmospheric plankton to observed signal returns at Ka-band frequencies probably should not have come as a surprise. In a series of papers from the late 1980s and early 1990s, Joseph R. Riley of the Radar Entomology Unit of the Natural Resources Institute, United Kingdom, and others made clear the value of 8-mm-wavelength radars in tracking insects. Unfortunately, it sometimes takes time for information to cross disciplinary boundaries.

8. The Active Remote Sensing of Clouds value-added product

In the early years of the ARM Program, the transitioning of software developed by scientists to operational applications within the ARM Program infrastructure was not a structured activity. Recognizing the need for operational radar processing, Eugene Clothiaux, working with ARM scientists Jimmy Voyles and David Turner in the early 2000s, created an initial operational version of the processing software of Clothiaux et al. (2000). Eventually, toward the middle of the decade, responsibility for the code was transferred to the ARM Program, where it continues to be maintained and developed. Under ARM Program guidance, the active remote sensing of clouds value-added product (ARSCL VAP) became the successful product that it has been and still is.

At its core, the ARSCL VAP contains the results of processing efforts to separate weak signals from noise, merge the different operational modes into holistic views of the vertical columns above the ARM sites, and mitigate the effects of atmospheric plankton (Fig. 17-3e). The primary goal of the ARSCL VAP, along with the MMCR, is to provide a high-temporal- (10 s) and spatial- (~45 m) resolution, long-term view of the vertical distributions of hydrometeors above the ARM sites. As noted in the article by Moran et al. (1998), the MMCR is intended for “climate research,” with the intent of mapping in time the macroscopic properties of clouds and the radar reflectivities associated with them.

The focus on macroscopic cloud properties is reflected in the ARSCL VAP. It contains a series of three height-versus-time cloud radar reflectivity (zero-Doppler moment) fields in units of decibels of reflectivity (i.e., Reflectivity, ReflectivityNoClutter, ReflectivityBestEstimate) that are a blend of the reflectivities from the different operational modes running on the MMCR and tuned to the detection of different cloud types. Each field is the result of additional processing applied to the reflectivities in order to identify clutter, with the parameter

ReflectivityBestEstimate representing the final outcome of the processing. The product also contains cloud-base heights versus time from a proprietary retrieval algorithm applied to laser ceilometer backscattering data (e.g., CloudBaseCeilometerStd), cloud-base heights (e.g., CloudBaseMplCloth to be replaced with CloudBaseMplZwang), and height-versus-time masks of all significant detections above molecular scattering (e.g., CloudMaskMplCloth to be replaced with CloudMaskMplZwang) from micropulse lidar backscattering data. Cloud-base heights retrieved from laser ceilometers and micropulse lidars are merged to form the best-estimate cloud-base height field CloudBaseBestEstimate. A series of fields called CloudLayerBottomHeights and CloudLayerTopHeights are derived from the ReflectivityBestEstimate field together with CloudBaseBestEstimate and one of the micropulse-lidar-derived cloud mask fields and represent the most succinct information on the time evolution of the vertical structure of clouds contained in the ARSCL VAP. In fact, the cloud-base height and cloud layer information contained in the main ARSCL VAP product are extracted from it and placed into two separate data products that contain files with much smaller sizes.

The ARSCL VAP also contains blended height-versus-time fields of the first (MeanDopplerVelocity) and second (SpectralWidth) radar Doppler moments, as well as a measure (SignaltoNoiseRatio) of the strengths of the returns leading to all three Doppler moments. Because many analyses benefit from knowing whether or not precipitation is reaching the surface, time series of a surface precipitation flag (CloudBasePrecipitation) were created from optical rain gauge data or a sensor on the microwave radiometers that detects liquid water.

Because interpolation of the operational mode datasets onto a single time grid is not optimal for all studies, the ARSCL VAP also contains a series of files that contain the original operational mode Doppler moments together with the CloudBaseBestEstimate field interpolated from the 10-s grid onto the operational mode time grid. These mode-based files also contain height-versus-time parameters called qc_RadarArtifacts and qc_ReflectivityClutterFlag. These two parameters contain flags constructed from the 10-s ARSCL VAP product and interpolated to the operational mode time grid that inform the user of issues in the individual mode data gleaned from an analysis of all of the mode data.

As we consider briefly at the end of the chapter, the MMCRs and the ARSCL VAP have gone a long way toward satisfying the intended purpose of providing useful observations on the macroscopic properties of

clouds and have expanded the reach of cloud radar data into modeling studies. However, every operational product that has value encourages use and increased scrutiny, which in turn leads to the discovery of additional problems and the desire for additional features. The result is an accumulation of an ongoing set of tasks to improve the process. This has certainly been our experience with the ARSCL VAP.

9. Fixing problems in the ARSCL VAP

By the mid-2000s plenty of ARSCL data files were available for scientists to analyze. As they did so, several problems with the ARSCL VAP were identified (e.g., Kollias et al. 2005). Among the more important problems were the following:

- 1) ARSCL VAP radar reflectivities were not calibrated.
- 2) Collection of water on the MMCR radome affected calibration in unknowable ways.
- 3) All MMCR modes (including the precipitation mode) were often saturated during precipitation events (Fig. 17-3d).
- 4) Scientific usability of the Doppler moments was compromised significantly by the long 9-s averages used to create them.
- 5) Atmospheric plankton contamination of the returns for the SGP site MMCR was so severe during the warm months (Fig. 17-3f) that it rendered long-term studies of boundary layer clouds at this site problematic.
- 6) Doppler moment accuracies were compromised by frequent velocity aliasing in the general mode (cf. Fig. 17-3g to Fig. 17-3h, in which positive, correct velocities in the “likely saturated” area of Fig. 17-3h have wrapped, or aliased, into incorrect negative velocities in the “velocity artifacts” area of Fig. 17-3g), boundary layer mode, and cirrus mode.
- 7) Doppler spectra during periods of strong returns had mirror images at oppositely signed Doppler velocities that, while 30 dB weaker than the desired returns, nonetheless corrupted the spectra sufficiently to preclude their use in cloud studies.
- 8) Doppler spectra had processing artifacts near zero Doppler velocities that made their use in cloud studies problematic.
- 9) Doppler moment accuracies were compromised by use of operational mode data in the final VAP that were from low signal-to-noise ratio measurements at times when other modes had higher signal-to-noise ratio measurements.

Inspection of this long list of issues with the MMCR output and associated ARSCL VAP might be viewed



FIG. 17-4. The waveguide from the NSA MMCR has worked its way free from its connection to the antenna port. This was a slow process that spanned many months of the harsh Arctic environment at the NSA site.

as a failure of the concept and/or its implementation. Not surprisingly, we have a very different perspective. For the first time, cloud radar signals ranging over seven orders of magnitude of returned power, from -50 to 20 dBZe (where dBZe is a popular unit for characterizing the power backscattered to a radar represented by the equivalent radar reflectivity factor Ze), were being scrutinized closely by scientists and engineers driven to use the results for understanding atmospheric processes at high resolution and in great detail. As a result of this scrutiny, sets of interlocking, often nonlinear, problems were found, resulting from a combination of technical (hardware) issues, software issues, computer limitations, and boundary layer meteorology. These issues were challenges that had to be overcome, one by one, to improve the ARM Program's capability to characterize cloud properties at each of its sites.

Each of the issues in the list above has served to launch efforts within the ARM Program to solve them and improve ARM radar products. As this process has evolved, the ARM Program's cloud radar activities have grown so that today the program is at the threshold of not only mapping the macroscopic properties of clouds but obtaining highly detailed information on cloud microphysical processes inside them as well. This evolution within the program is best illustrated by consideration of

how these problems have been addressed and solved within the program.

10. Calibrating vertically pointing cloud radars

From the beginning of the ARM Program, calibration of the cloud radars has been a key consideration. The first version of the MMCR contained hardware for closely monitoring the transmit power and injecting a noise signal into the receiver as part of normal operations. However, this left several passive radio-frequency components and the antenna out of the calibration loop. The ARM Program's radar engineers periodically measured the loss in these radio-frequency components during annual site visits. Typically, the MMCR antennas were thoroughly characterized once in their life cycle just after their manufacture. However, it was not possible to measure the performances (e.g., gain, beamwidth, cross-polarization isolation, etc.) of these 2–3-m-diameter Cassegrain antennas in the field. Attempts were made to place calibration targets (e.g., BBs, ball bearings shot out of a paintball gun, and dangling a metallic sphere under a helicopter) in the radar beam. However, with only 0.3° beam widths, getting these targets into exact regions within the radar field of view is extremely difficult and certainly not feasible on a routine basis.

In 2004, the ARM Program began the procurement of the WACR (Fig. 17-2b) to be collocated with the MMCR. Because the WACR had a much smaller (24-in diameter) antenna, a splash plate was incorporated into its design so that its beam could be deflected to point at a trihedral corner reflector target. For the first time, the ARM Program gained the capability to calibrate one of its radars with an external calibration target that had a known reflectivity value.

An example of why it is important to calibrate with an external target was evidenced by a component failure at the ARM NSA site in Barrow, Alaska, during 2006 through 2007. In addition to being in a harsh Arctic environment with severe cold, the radar is sited 600 m from a saltwater lagoon. Corrosion slowly acted on the waveguide that was attached to the antenna feed, eventually breaking the machine screws that attached the waveguide to the feed (Fig. 17-4). This was such a slow process that diminishing radar returns went unobserved until an ARM radar engineer arrived at the site for an inspection. He was amazed that the radar was detecting any return power at all!

This inability to calibrate a vertically pointing MMCR is perhaps its greatest weakness. This problem was recognized during the early design discussions in the 1990s, but no one realized that it would be such a significant,

insidious problem for operational cloud radars, because there were no such systems at the time. The possibility of scanning the cloud radar (for both calibration and science) was considered but was dropped, because it was a significant challenge to build an operational vertically pointing system in itself, scanning hardware was expensive and operationally problematic at the remote sites,² and slow operational degradation was not seen as a critical issue. (Degradation of the power source was considered, but there were ways to monitor this process without the need for a total system calibration via calibration target measurements.) The view now shared widely across the program is that calibration is about proving to oneself that every piece of the radar is working and, to the extent that a piece is not working optimally, quantifying the impact of that degradation on the overall estimates of the power backscattered by hydrometeors within each radar sample volume. In retrospect, this view should have been implemented much earlier, but it is unclear how the program could have addressed this problem during its first decade of operations, given the limitations and cost of scanning technology at the time.

These painful lessons about calibration have not been lost on the program. In January 2011, the SGP MMCR was replaced with the new KAZR (which is similar in outward appearance to the MMCR, as Fig. 17-2a illustrates). By itself, the KAZR, like the MMCR, cannot be calibrated from the antenna to the receiver. But every deployment of a KAZR will come with the deployment of a dual-frequency Scanning ARM Cloud Radar (SACR; Fig. 17-2c), one frequency of which is in the Ka band. At the SGP site, the first Ka-band SACR (Ka-SACR) was deployed in May 2011. The program has adopted the view that the deployment of every SACR must include placement of a corner reflector nearby. The SACRs will be calibrated both internally via transmitter and receiver measurements and externally via corner reflector measurements. The calibration of the SACRs will then be transferred to the calibration of the KAZRs, with comparisons of the SACR calibration to the KAZR's internal transmitter and receiver measurements used to identify problems with the KAZR that require referencing in some way to measurements from a known target.

²The discussions at the time included the trade-off among antenna size, radar sensitivity, and pointing (or scanning). The SGP Ka band with its 10-ft antenna dish was designed to achieve maximum sensitivity to low hydrometeor concentrations, and it was enormously successful from that perspective. But the large size of the antenna precluded pointing because of weight and cost, not to mention the question of alteration in the antenna shape if it were tipped from horizontal to vertical orientation.

In the fall of 2012, the ARM Program radar operations and engineering group reported its first findings using corner reflector measurements to calibrate the SACRs. The findings were promising. By scanning across the corner reflector using a set of stacked raster scans, they were not only able to estimate overall SACR calibration but were also able to map out rough outlines of the antenna beam pattern. In this way, they were able to identify problems with the SACR antenna first deployed to the Two-Column Aerosol Project (TCAP) on Cape Cod, Massachusetts. They were also able to use corner reflector measurements to track in time the impacts of icy precipitation on the SGP SACR's performance. As ice accumulated on the SACR's radome, attenuation increased, and the beam pattern of the SACR changed considerably. As the ice melted and the radome dried out, they were able to watch the SACR return to nominal operating characteristics. As a result of these early successes, corner reflector raster scans are being implemented as part of normal SACR scanning operations on a time scale sufficiently fine to track changes in calibration during precipitation events.

11. Avoiding cloud radar reflectivity saturation from precipitation

The amount of radar signal power backscattered from a single spherical liquid drop that is small compared to the radar wavelength is approximately proportional to the drop diameter to the sixth power. The total power backscattered from a collection of spherical drops all the same size is the number of drops in the illuminated volume times the backscattered power per drop. Consider a liter of air with one precipitating drop with a diameter of 1 mm and 10^5 cloud droplets each with a diameter of $10\ \mu\text{m}$. The ratio of the power backscattered by the single precipitating drop to that from all of the cloud droplets is 10^7 . (Is that not amazing? One precipitating drop backscatters 10^7 more power than 10^5 cloud droplets.) Another challenge to consider is that the MMCR is sensitive to echoes as weak as $-50\ \text{dBZe}$, and their intensity can reach $20\ \text{dBZe}$. But accurately measuring the power over such a dynamic range is no easy engineering task to accomplish (consider holding a single penny versus 10^7 of them), and the MMCR saturates on the high end of this power range. Each time a return power saturates the receiver, the bias in the estimate (in this case underestimation) of the returned power increases.

To mitigate this problem, the return power to the radar needs to be reduced by a known amount before it gets to the hardware in the receiver that saturates. In 2004, at a meeting at the NOAA Environmental Technology

Laboratory (now known as the NOAA Earth System Research Laboratory in Boulder, Colorado, ARM Program and NOAA radar engineers and scientists agreed on a possible mitigation strategy. The MMCR receiver has four switches that protect it during transmission of the high-power pulse. During transmission, the switches are closed, and any power that leaks from the transmitter into the receiver is blocked. When a transmit pulse has cleared the radar, the switches are opened, allowing backscattered power from the atmosphere to enter the radar receiver. Each switch attenuates signals by an amount of 20–25 dB. It was decided to create a new operational mode whereby one of the switches was kept closed (protection mode) even when the radar received signals from the atmosphere. By keeping the switch closed, the received atmosphere signal was attenuated by an amount equal to 20–25 dB, thereby extending the MMCR receiver dynamic range by 20–25 dB. Knowing how much the signal was attenuated by the switch, an equal amount was added during data postprocessing, thus producing a calibrated reflectivity. This approach was implemented only during the operation of the MMCR precipitation mode and was put into operation within the MMCRs at the SGP and TWP sites over the period from mid-2004 through mid-2006. After a period of experimentation, during which time the precipitation mode data of the MMCR's with the innovation were corrupted by timing issues, this approach was implemented successfully, and the quality of the precipitation mode data was vastly improved.

Leaving a switch closed in the precipitation mode when the radar was receiving atmospheric returns is a clever, but not elegant, solution to saturation. Despite the additional protection, the MMCR receiver still saturated in heavy precipitation (above 5 mm hr^{-1}). As importantly, the software (ARSCL) that was designed to select the mode with the highest signal-to-noise ratio (SNR) was never adjusted to routinely select the lower SNR but nonsaturated, radar reflectivities of the precipitation mode.

In the design of the new KAZRs and SACRs, saturation of the receiver during periods of heavy precipitation is dealt with more elegantly. The KAZR features an improved radar receiver and a larger dynamic range for the signal powers within it; thus, its nominal saturation level is 15 dB higher than that of the MMCR (see [Table 17-2](#)). This is, of course, not enough. The current plan is to implement amplitude tapering on the transmitted pulse to reduce the return signal power. In addition, the ARM Program has strengthened its ability to profile precipitation by collocating 915-MHz radar wind profilers with the profiling cloud radars ([Tridon et al. 2013](#)).

Over the years, interactions between scientists using ARM radar data (and identifying problems within it) and ARM radar engineers have led to substantially improved radar systems. These interactions are no less important going forward, given the growth of the number of radars in the ARM Program and the complexity of the radar data products produced by them.

12. The rise of the digital receiver: Temporal resolution and Doppler spectra

In the early design and implementation of the ARM cloud radars, the need for continuous and robust operations of the MMCR led to a decision to use two digital signal processors (DSPs) based on those in use by the NOAA wind-profiler network along with the OS/2 operating system-based profiler online program (POP) software that came with them. The POP was the standard wind-profiler processor that provided reliable moments data (i.e., reflectivities, Doppler velocities, and spectral widths) but at a low collection efficiency (5%–30%). The initial temporal resolution of the MMCR data was 9 s; however, most of the time in the 9-s window was dedicated to signal processing rather than signal integration, which is the definition of low efficiency. This initial choice of the DSP and POP software, made largely for reasons of cost and a shorter development cycle, eventually led to issues that created strong pressure for innovation.

The pressure for innovation was driven by several significant science issues. The 9-s temporal resolution of the original MMCR Doppler moments was dictated by the need for averaging in order to increase the SNR of the measurements and to keep the data volume down. The emphasis on SNR was again in response to the need for sensitivity in support of cloud macrophysical studies. The time interval and the data volume restrictions, however, were driven by the available computer technology in the 1990s. The cost of computer power, especially data storage and networking, was much higher early in the 1990s. Despite the data limitations, several ARM scientists were eager for higher-resolution data both in time and in spectral space because they recognized the research potential of these data. For example, [Kollias et al. \(2001\)](#) demonstrated that 1-s temporal resolution was required for dynamical studies of updrafts, downdrafts, and turbulence in fair weather cumuli. Additional research by [Kollias et al. \(2005\)](#) demonstrated the importance of time scales shorter than 9 s that could only be captured by a more efficient processor. These science considerations, together with the availability of more capable radar and computer hardware, led to a processor upgrade effort that was undertaken in the period from 2003 to 2005.

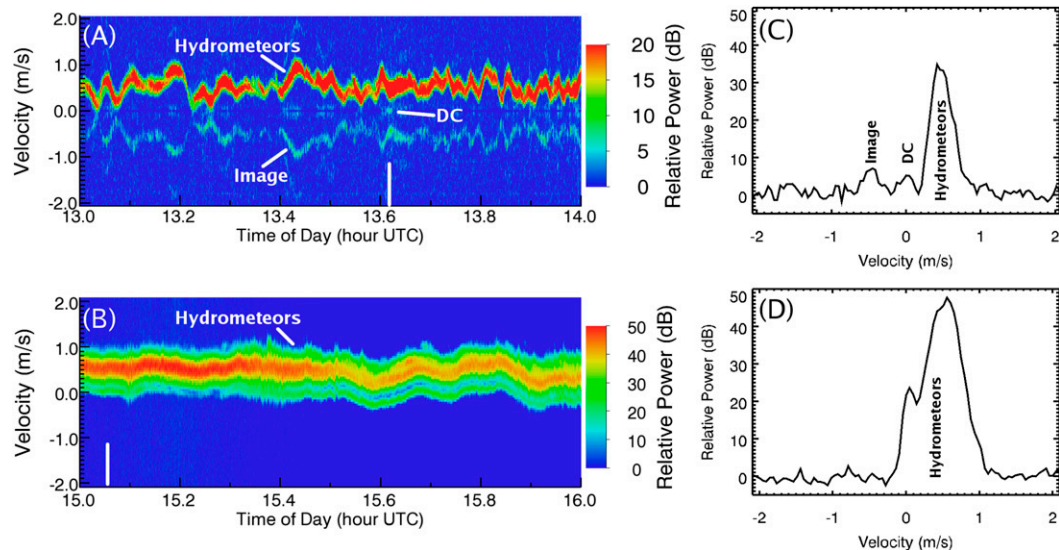


FIG. 17-5. (a) Example of an MOCR Doppler spectrogram collected over 1 h at constant height in a cloud at the NSA in 2009. (b) Example of a KAZR Doppler spectrogram collected over 1 h at constant height in a cloud at the NSA in 2012. (c) One of the Doppler spectra shown in (a), but as relative power vs velocity. The spectral image is labeled as “image” in this figure and is not the result of any physical phenomena in the atmosphere; rather, the spectral image results from hydrometeor contributions to powers in the spectrum at positive velocities artificially bleeding into powers at negative velocities because of imperfections in the radar receiver. (d) One of the KAZR Doppler spectra shown in (b), but as relative power vs velocity.

With support from the ARM Program and NOAA, Radian, Inc., (subsequently purchased by Vaisala) began the design of a new DSP board for the MOCR. The new board, based on the C-40 DSP from Texas Instruments, was a five-DSP-on-the-board processor. The advantages of the new design were the use of higher clock frequencies and multiple DSPs working in parallel to accelerate radar processing power. The hardware ran under a new radar control software program called Lower Atmosphere Profiler—Extensible Markup (LAP-XM), which in turn ran in the Windows 2000 environment. This new processor was eventually installed at the SGP and NSA sites as well as on the NOAA MOCR that was deployed to Eureka, Canada. The processor efficiency of the new board was 50%. Unfortunately, Texas Instruments manufactured only three such processor boards before this line was discontinued.

Around the same time that the C-40 was discontinued, the National Center for Atmospheric Research licensed its PC-Integrated Radar Acquisition System (PIRAQ-III) technology to Vaisala. The new PIRAQ-III was selected as the upgrade for the TWP sites. The benefit of the PIRAQ-III was that the boards and software were supported products of Vaisala (Widener et al. 2004). Moreover, the processor efficiency of the PIRAQ-III was close to 70%, an improvement over the C-40 processors. The first PIRAQ-III upgrade was completed at Darwin in November 2005. The upgrades for Manus and Nauru were

completed the following year. In an attempt to enhance processor efficiency for the NSA Indirect and Semi-Direct Aerosol Campaign (ISDAC; McFarquhar et al. 2011) in April 2008, the C-40 processor at NSA, which was installed just before the NSA Mixed-Phase Arctic Cloud Experiment (M-PACE; Verlinde et al. 2007) in October 2004, was replaced by a PIRAQ-III in December 2007.

During the same period from 2004 to 2005, the MOCR sampling modes were revised. The new modes introduced wider velocity ranges for the Doppler spectra and shorter (1.5 s) integration times. Most importantly, the ARM Program started to record radar Doppler spectra on more than a case-study basis. Preliminary analysis of Doppler spectra recorded by the C-40 and PIRAQ-III boards showed the presence of spectral images when the peak spectral power was higher than 25–30 dB above the noise (Fig. 17-5). This artificial feature was a real nuisance to radar meteorologists and scientists who used the Doppler spectra for cloud microphysical retrievals. As it turned out, features like this in the NSA ISDAC PIRAQ-III Doppler spectra rendered them no better, and often far worse, than the NSA MPACE C-40 Doppler spectra.

As MOCR Doppler spectra became available throughout the mid-2000s, the scientists who analyzed them found that they contained a wealth of information, especially regarding the study of precipitating liquid drops and ice crystals in the presence of cloud liquid

water droplets. But there were two problems in the MMCR Doppler spectra that immediately became apparent: removal of low-level constant voltages within the radar receiver led to artifacts near zero-Doppler velocities, and strong power returns from downward-moving precipitating particles led to spurious powers showing up at oppositely signed Doppler velocities. These spurious power returns were called spectral images (see Fig. 17-5c). While these images were often 30 dB down (or one one-thousandth) in power of the actual returns from precipitating particles, they often fell at Doppler velocities where cloud power returns occurred. As a consequence, the Doppler spectra were compromised for study of cloud power returns, which require either no images in the Doppler spectra or ones that are at least 40 dB down (or one ten-thousandth) in power.

13. The WACR as a test bed for future MMCR improvements

While the MMCR digital receiver upgrade saga was unfolding, a parallel effort from 2003 to 2005 was underway to acquire a 94-GHz (W band) radar at the ARM SGP site. The WACR acquisition was motivated by the need to improve detectability of clouds in the boundary layer at the ARM SGP site during the warm season, a period when insect echoes were making the qualitative and quantitative estimation of hydrometeor returns very challenging.

The improved capability of W-band radars to separate hydrometeor returns from those of insects is based on the suppression of the insect radar returns by 20 dB compared to the MMCR because of the drop in back-scattered powers (in this case, from the insects) as their sizes approach and exceed the radar wavelength (Luke et al. 2008). Several of the authors of this chapter were present in an intense meeting that took place at one of the DOE laboratories in 2004 to decide on the utility of a WACR as an insect-free radar. The determination of the ARM chief scientist at the time, Thomas Ackerman, played a critical role in the final decision to build and deploy the WACR. Preliminary comparison of WACR and MMCR reflectivities at the SGP site in 2005 demonstrated that a 94-GHz radar has excellent sensitivity, suppresses the clear-air clutter from insects, and is highly sensitive to weak returns from boundary layer clouds and cirrus layers.

However, this is just half of the story. Unlike the MMCR, the WACR does not use pulse coding and operates in only copolarization [transmits H polarization and receives H-polarization radiation in a general (GE) mode] and cross-polarization [transmits H

polarization and receives V polarization in a polarization (PO) mode], each with a 2-s integration, or dwell, time. Having fewer (two) modes eased the development of the WACR ARSCL VAP compared to the MMCR ARSCL VAP, which merges six modes over a span of 16 s. The frequent repetition of the cross-polarization mode and the suppression of the insect returns made the development of an automated insect filtering algorithm possible. Furthermore, the WACR had a sophisticated internal calibration mode, an intermediate-frequency (IF) digital receiver with 100% data efficiency, and produced high-quality radar Doppler spectra with no artifacts.

If we knew in advance the many different ways the acquisition of the WACR would benefit the ARM Program cloud radar, the decision for its acquisition in 2004 would have been easier. However, the future evolution of the ARM Program's cloud radars was clear: it was to be based on an evolution of WACR technology.

14. Doppler moments from spectra with complications

For MMCR processing, Doppler moments computed from Doppler spectra with velocity aliasing are problematic because the radar's processing does not account for the velocity aliasing. Doppler moments computed from Doppler spectra with both precipitation and cloud drops are problematic in that the Doppler moments characterize simultaneously the return powers from both of them and not the properties of each of the two separate types of drops individually. If return powers from atmospheric plankton make significant contributions to the Doppler spectra, the Doppler moments that result from them contain information from both hydrometeors and the plankton. To address all of these problems there is one way forward: collect the spectra so that detailed investigations of the spectra can lead to methods for processing them that remove all of these problems (or at least reduce them to a manageable level). In support of this goal, the ARM Program started collecting MMCR spectra continuously as the MMCR C-40 and MMCR PIRAQ-III upgrades were made and collecting WACR spectra in late 2005, extending this procedure to all KAZR and SACR Doppler spectra obtained while the radars are pointing vertically.

These Doppler spectra have been put to their intended purposes. Luke et al. (2008) demonstrated that a neural network trained on insect contributions to Doppler spectra is successful in identifying insect contributions to novel Doppler spectra in about 92% of cases. They further demonstrated that, when polarization information is included in the analysis of Doppler

spectra, detection of atmospheric plankton gets even better. At the same time, Kollias et al. (2007b) showed that availability of Doppler spectra makes analysis of velocity aliasing, multiple hydrometeor phase or size spectrum contributors to the return power, and other features possible, thereby providing a path to much improved Doppler moments. Ongoing efforts within the ARM Program have expanded upon the study of Kollias et al. (2007b), leading to novel processing strategies that will use polarization-diverse Doppler spectra to mitigate past processing issues in creation of the Doppler moments.

Implementation of many of the ARM Program's new strategies requires access to Doppler spectra and then processing each and every one of them. Doppler spectra from the MMCRs, KAZRs, and SACRs now fill the ARM data archive with upward of 150 TB of data. This staggering amount of data places constant stress on collection, transmission, and storage technologies and will continue to increase in size with each passing day of ARM cloud radar operations. That said, modern technology brings many novel techniques to deal with these extremely large datasets. Ed Luke adapted one of them—graphics processing units (GPUs)—to the processing of radar Doppler spectra. With the implementation of his new processing strategies on the GPUs they can work their way through the entire ARM data archive holdings of Doppler spectra within a month of wall clock time. In addition to processing power, Ed Luke developed a sophisticated radar Doppler spectra visualization and analysis toolkit that enhances the ability of scientists to access, analyze and synthesize radar Doppler spectra from multiple radars and other ARM data (http://www.gim.bnl.gov/armclouds/specvis_java_toolkit/).

15. The fourth-generation MMCR, or KAZR, and the new KA/W/X-SACRs

From the first day of MMCR operations at the ARM SGP site, our community has been on a steep learning curve related to the challenges of continuous operations and data processing. The sluggish pace in MMCR digital receiver hardware and software upgrades between 1996 and 2011, which could not run ahead of technological advances, provided time to focus on these challenges not directly associated with the radar itself. However, propelled by the experience acquired over the last 18 years, advances in technology, and the boost to the radar infrastructure through the American Recovery and Reinvestment Act of 2009 (Mather and Voyles 2013), ARM has enhanced its cloud and precipitation observational capabilities and is again facing a daunting

challenge as it attempts to operate dozens of radars and process the complex data from them. Kevin Widener, the leader of the ARM radar operations and engineering group at the time, was instrumental in managing the complex process of developing technical specifications, going through the public tender, and acquiring, testing and deploying these new ARM cloud radars.

The MMCR was replaced with the ProSensing, Inc., KAZR. The new KAZR uses several of the core technologies and capabilities of the MMCR: 1) the travel wave tube amplifier (TWTA) technology, 2) the frequency (35-GHz), 3) some of the radio-frequency (RF) electronics, 4) the antenna, and 5) the environmental enclosure. The biggest improvement in the KAZR relative to the MMCR can be found in the new digital receiver that replaces the C-40 and PIRAQ-III receivers, enabling the KAZR to transmit sophisticated long-pulse waveforms with pulse compression along with short pulses for probing the lower atmosphere. Along with superior-quality radar Doppler spectra free of image artifacts (Fig. 17-5) and higher 1-s temporal resolution, the KAZR provides researchers with the capability to study cloud dynamics and microphysics using the recorded radar Doppler spectra (e.g., Kollias et al. 2011).

In addition to the upgrades to the vertically profiling cloud radar, the ARM Program acquired eight SACRs that were developed and fabricated by ProSensing, Inc. The SACRs are sophisticated, dual-frequency (five SACRs have Ka/W-band frequency pairs and three have Ka/X-band frequency pairs) radar systems mounted on a single pedestal (Fig. 17-2c). The Ka/W-SACRs are intended mostly for midlatitude and Arctic regions where the impact of attenuation by atmospheric water vapor is less severe than in the tropics. The beams of the Ka- and W-band radars within an SACR are almost matched to each other and very narrow (less than 0.33°). Contrary to the KAZR, the Ka/W-SACR uses a relatively high-power extended interaction klystron amplifier (EIKA) transmitter with peak power over 1.6 kW. The Ka- and W-band radar systems have dual polarization but only transmit horizontal polarization states and receive signals in both horizontal and vertical polarization states. The last two of the eight Ka/W-SACR systems came online in 2015 and are fully polarization diverse; that is, they transmit both horizontal and vertical polarization states (though not simultaneously) and measure both horizontal and vertical polarization returns, which are invaluable for the study of ice clouds.

The Ka/W-SACRs use a digital waveform generator capable of producing arbitrary waveforms, which enables the use of frequency diversity and pulse compression waveforms. They use spectral processing for filtering and parameter estimation. The systems routinely store the

full Doppler spectrum when operating in zenith-pointing mode and are capable of storing the base-band in-phase and quadrature-phase signals. They use corner reflector targets located on towers at a range of 400–500 m for calibration of themselves and the nearby KAZRs and/or WACRs. They can be remotely configured and have been designed to implement adaptive scanning strategies (Kollias et al. 2014).

The X/Ka-SACRs are mostly geared toward tropical regions where atmospheric water vapor will not have as severe an impact on X- and Ka-band beams as compared to a W-band beam. The beams of the X- and Ka-band radars are not matched to each other. The X-SACRs use a much (about 3.5 times) wider beam compared with the Ka-SACR, as mounting an X-band antenna with a 0.33° beamwidth (comparable to that of a Ka-SACR) on the same pedestal is not practical. Their receiver and transmitter units are antenna mounted, which results in low power losses in the radio-frequency sections of the transmitter and receiver. The X-SACRs are fully polarimetric, simultaneously transmitting and receiving both horizontal and vertical polarization states.

The SACRs are the primary instruments for the detection of cloud properties (boundaries, water contents, dynamics, etc.) beyond the vertical columns directly above the ARM sites. Having scanning capabilities with two frequencies and polarization allows for more accurate probing of a variety of cloud systems (e.g., drizzle and shallow, warm rain), better correction for attenuation, use of attenuation for liquid water content retrievals, polarimetric characterization of nonspherical particles, and habit identification.

16. Reprocessing of the ARSCL VAP and wind profilers as part of cloud observations

The last file produced by the SGP MMCR occurred in January 2011, that for the NSA MMCR in March 2011, and those for the TWP MMCRs in February and March 2011. The lifetime of the MMCRs within the ARM Program spanned November 1996 through March 2011 for a total approaching 15 years. Its record within the ARM Program is now complete.

In May 2013, the ARM Program organized a meeting to discuss all the problems and issues in MMCR data and its related ARSCL VAP. The suboptimal ways in which the operational modes of the MMCRs were merged into the ARSCL VAP were discussed and ways to improve the merging considered. Newer, better methods for assessing the quality of MMCR mode data emerged as a result.

One set of ideas put forth in the meeting showed how specific consistency checks between different MMCR modes could be used to identify saturation within the

MMCR receiver for that mode. Knowing whether or not a mode is saturated provides important information on the quality of the mode data and its suitability for inclusion within the ARSCL VAP (Galletti et al. 2014). The last question remaining in this investigation is whether or not saturation can be detected in the precipitation mode itself, both before and after the switch approach to mitigating saturation was implemented.

Another set of ideas put forth by several of the participants of the meeting demonstrated that there is simply no way to assess attenuation in real time through the MMCR radome and atmosphere above without measurements at lower nonattenuating (i.e., wind profiler) wavelengths (Tridon et al. 2013). These arguments further strengthen the arguments for placing a 915-MHz wind profiler and a disdrometer beside each KAZR and SACR pair in order to complete the instrument package with today's technology that can best be used to probe atmospheric hydrometeors. It is conceivable that, in the future, the wind profiler will become one of the key input data streams to the ARSCL VAP.

Once the ARM cloud radar program resolves the issues related to the quality of data from each mode and how best to handle attenuation in real time, it will be time to reprocess the ARSCL VAP in its entirety. The complete MMCR dataset, its overall quality, and the quality of the related ARSCL VAPs for all sites and times that emanate from the reprocessing will be discussed in a review article. This article will represent the definitive statement on the quality of the MMCR data record within the ARM Program.

17. Closing remarks

The ARM Program's decision to invest in the relatively new and immature technology of millimeter-wavelength cloud radars was both bold and brave. This decision was based on the determined advocacy of a small group of ARM scientists and engineers³ backed up by a handful of scientific studies using data primarily from research radars built and operated by groups at the Pennsylvania State University (Thomas Ackerman, Bruce Albrecht, and colleagues), the University of Massachusetts (Robert McIntosh, James Mead, and colleagues), and the NOAA Environmental Research Laboratory (Robert Kropfli, Kenneth Moran, and colleagues). In retrospect, it may

³ A number of the authors of this chapter were members of that group. We would like to acknowledge the contributions of the late Dr. Robert McIntosh of the University of Massachusetts and Dr. Robert Kropfli of NOAA Environmental Technology Laboratory (ETL) to the initiation of and support for the ARM radar program.

seem that it was an easy decision, but at the time there were serious questions about the reliability of millimeter-wavelength technology, the high cost of building instruments for which there were no commercial vendors, and the extent to which continuous cloud radar data could be collected and used. Development, particularly of processing and storage software, was challenging because of unexpected problems and sometimes slower than hoped. ARM Program management is to be congratulated for persevering in its vision to deploy cloud radars to its sites in spite of these difficulties.

The operation of the ARM millimeter-wavelength cloud radars beginning in 1996 and continuing to the present has provided the scientific community with an unprecedented quantitative view of cloud properties and processes over the ARM fixed sites and the new mobile facilities. To those of us who remember the excitement of acquiring a few hours of continuous millimeter-wavelength radar data during a field campaign, this wealth of radar data is truly stunning. The nearly 15 years of MMCR observations, now being extended by the new generation of radars, have been critically important in advancing our capability to evaluate model simulations, develop and evaluate cloud parameterizations, and provide key insights into cloud processes that are central to the climate modeling puzzle.

While discussion of cloud property retrievals and their use in model process and parameterization development is beyond the scope of this chapter, these topics are the focus of [Shupe et al. \(2016, chapter 19\)](#). Moreover, accessible discussions on liquid cloud, ice cloud, and mixed-phase cloud property retrievals can be found in the articles by [Turner et al. \(2007\)](#), [Comstock et al. \(2007\)](#), and [Shupe et al. \(2008\)](#), with many other published articles highlighting the importance of cloud radar data in this ongoing process (e.g., [Botta et al. 2011](#); [Deng and Mace 2006](#); [Dong and Mace 2003](#); [Frisch et al. 1995](#); [Kollias et al. 2001, 2002, 2007a, 2011](#); [Luke et al. 2010](#); [Luke and Kollias 2013](#); [Matrosov et al. 2012](#); [O'Connor et al. 2005](#); [Shupe et al. 2004](#)).

The development and advancement of millimeter-wavelength radar hardware and software components and support for scientific use of radar data are a lasting legacy of the ARM Program. There is no doubt that the ARM Program played the leading role in this field for the past 20 years. Its new radars that are now being integrated into the fixed sites and mobile facilities are evidence that the ARM Program expects to sustain its leadership role. Although there have been many obstacles to reaching the full potential of millimeter-wavelength cloud radars, our vision for the role that these radars could and should play in atmospheric cloud research and improving climate simulations is being realized.

REFERENCES

- Ackerman, T. P., and G. M. Stokes, 2003: The Atmospheric Radiation Measurement Program. *Phys. Today*, **56**, 38–44, doi:[10.1063/1.1554135](#).
- Albrecht, B. A., C. S. Bretherton, D. Johnson, W. H. Schubert, and A. S. Frisch, 1995: The Atlantic stratocumulus transition experiment—ASTEX. *Bull. Amer. Meteor. Soc.*, **76**, 889–904, doi:[10.1175/1520-0477\(1995\)076<0889:TASTE>2.0.CO;2](#).
- Botta, G., K. Aydin, J. Verlinde, A. E. Avramov, A. S. Ackerman, A. M. Fridlind, G. M. McFarquhar, and M. Wolde, 2011: Millimeter wave scattering from ice crystals and their aggregates: Comparing cloud model simulations with X- and Ka-band radar measurements. *J. Geophys. Res.*, **116**, D00T04, doi:[10.1029/2011JD015909](#).
- Cess, R. D., and Coauthors, 1990: Intercomparison and interpretation of climate feedback processes in 19 atmospheric general circulation models. *J. Geophys. Res.*, **95**, 16 601–16 615, doi:[10.1029/JD095iD10p16601](#).
- Clothiaux, E. E., M. A. Miller, B. A. Albrecht, T. P. Ackerman, J. Verlinde, D. M. Babb, R. M. Peters, and W. J. Syrett, 1995: An evaluation of a 94-GHz radar for remote sensing of cloud properties. *J. Atmos. Oceanic Technol.*, **12**, 201–229, doi:[10.1175/1520-0426\(1995\)012<0201:AEOAGR>2.0.CO;2](#).
- , T. P. Ackerman, G. G. Mace, K. P. Moran, R. T. Marchand, M. A. Miller, and B. E. Martner, 2000: Objective determination of cloud heights and radar reflectivities using a combination of active remote sensors at the ARM CART sites. *J. Appl. Meteor.*, **39**, 645–665, doi:[10.1175/1520-0450\(2000\)039<0645:ODOCHA>2.0.CO;2](#).
- Comstock, J. M., and Coauthors, 2007: An intercomparison of microphysical retrieval algorithms for upper-tropospheric ice clouds. *Bull. Amer. Meteor. Soc.*, **88**, 191–204, doi:[10.1175/BAMS-88-2-191](#).
- Danne, O., G. G. Mace, E. E. Clothiaux, X. Dong, T. P. Ackerman, and M. Quante, 1996: Observing structures and vertical motions within stratiform clouds using a vertical pointing 94-GHz cloud radar. *Contrib. Atmos. Phys.*, **69**, 229–237.
- Deng, M., and G. G. Mace, 2006: Cirrus microphysical properties and air motion statistics using cloud radar Doppler moments. Part I: Algorithm description. *J. Appl. Meteor. Climatol.*, **45**, 1690–1709, doi:[10.1175/JAM2433.1](#).
- Dong, X., and G. G. Mace, 2003: Profiles of low-level stratus cloud microphysics deduced from ground-based measurements. *J. Atmos. Oceanic Technol.*, **20**, 42–53, doi:[10.1175/1520-0426\(2003\)020<0042:POLLSC>2.0.CO;2](#).
- Ecklund, W. L., C. R. Williams, and P. E. Johnston, 1999: A 3-GHz profiler for precipitating clouds. *J. Atmos. Oceanic Technol.*, **16**, 309–322, doi:[10.1175/1520-0426\(1999\)016<0309:AGPFPC>2.0.CO;2](#).
- Ellingson, R. G., and W. J. Wiscombe, 1996: The Spectral Radiance Experiment (SPECTRE): Project description and sample results. *Bull. Amer. Meteor. Soc.*, **77**, 1967–1985, doi:[10.1175/1520-0477\(1996\)077<1967:TSREPD>2.0.CO;2](#).
- , R. D. Cess, and G. L. Potter, 2016: The Atmospheric Radiation Measurement Program: Prelude. *The Atmospheric Radiation Measurement (ARM) Program: The First 20 Years*, Meteor. Monogr., No. 57, Amer. Meteor. Soc., doi:[10.1175/AMSMONOGRAPHS-D-15-0029.1](#).
- Frisch, A. S., C. W. Fairall, and J. B. Snider, 1995: Measurement of stratus cloud and drizzle parameters in ASTEX with a Ka-band Doppler radar and a microwave radiometer. *J. Atmos. Sci.*, **52**, 2788–2799, doi:[10.1175/1520-0469\(1995\)052<2788:MOSCAD>2.0.CO;2](#).

- Galletti, M., D. Huang, and P. Kollias, 2014: Zenith/nadir pointing mm-wave radars: Linear or circular polarization? *IEEE Trans. Geosci. Remote Sens.*, **52**, 628–639, doi:[10.1109/GRS.2013.2243155](https://doi.org/10.1109/GRS.2013.2243155).
- Keenan, T., and Coauthors, 2000: The Maritime Continent Thunderstorm Experiment (MCTEX): Overview and some results. *Bull. Amer. Meteor. Soc.*, **81**, 2433–2455, doi:[10.1175/1520-0477\(2000\)081<2433:TMCTEM>2.3.CO;2](https://doi.org/10.1175/1520-0477(2000)081<2433:TMCTEM>2.3.CO;2).
- Kollias, P., B. A. Albrecht, R. Lhermitte, and A. Savtchenko, 2001: Radar observations of updrafts, downdrafts, and turbulence in fair-weather cumuli. *J. Atmos. Sci.*, **58**, 1750–1766, doi:[10.1175/1520-0469\(2001\)058<1750:ROOUDA>2.0.CO;2](https://doi.org/10.1175/1520-0469(2001)058<1750:ROOUDA>2.0.CO;2).
- , —, and F. Marks Jr., 2002: Why Mie? Accurate observations of vertical air velocities and raindrops using a cloud radar. *Bull. Amer. Meteor. Soc.*, **83**, 1471–1483, doi:[10.1175/BAMS-83-10-1471](https://doi.org/10.1175/BAMS-83-10-1471).
- , E. E. Clothiaux, B. A. Albrecht, M. A. Miller, K. P. Moran, and K. L. Johnson, 2005: The Atmospheric Radiation Measurement program cloud profiling radars: An evaluation of signal processing and sampling strategies. *J. Atmos. Oceanic Technol.*, **22**, 930–948, doi:[10.1175/JTECH1749.1](https://doi.org/10.1175/JTECH1749.1).
- , —, M. A. Miller, B. A. Albrecht, G. L. Stephens, and T. P. Ackerman, 2007a: Millimeter-wavelength radars: New frontier in atmospheric cloud and precipitation research. *Bull. Amer. Meteor. Soc.*, **88**, 1608–1624, doi:[10.1175/BAMS-88-10-1608](https://doi.org/10.1175/BAMS-88-10-1608).
- , —, —, E. P. Luke, K. L. Johnson, K. P. Moran, K. B. Widener, and B. A. Albrecht, 2007b: The Atmospheric Radiation Measurement Program cloud profiling radars: Second-generation sampling strategies, processing, and cloud data products. *J. Atmos. Oceanic Technol.*, **24**, 1199–1214, doi:[10.1175/JTECH2033.1](https://doi.org/10.1175/JTECH2033.1).
- , J. Rémillard, E. Luke, and W. Szyrmer, 2011: Cloud radar Doppler spectra in drizzling stratiform clouds: 1. Forward modeling and remote sensing applications. *J. Geophys. Res.*, **116**, D13201, doi:[10.1029/2010JD015237](https://doi.org/10.1029/2010JD015237).
- , N. Bharadwaj, K. Widener, I. Jo, and K. Johnson, 2014: Scanning ARM cloud radars. Part I: Operational sampling strategies. *J. Atmos. Oceanic Technol.*, **31**, 569–582, doi:[10.1175/JTECH-D-13-00044.1](https://doi.org/10.1175/JTECH-D-13-00044.1).
- Lhermitte, R. M., 1966: Probing air motion by Doppler analysis of radar clear air returns. *J. Atmos. Sci.*, **23**, 575–591, doi:[10.1175/1520-0469\(1966\)023<0575:PAMBDA>2.0.CO;2](https://doi.org/10.1175/1520-0469(1966)023<0575:PAMBDA>2.0.CO;2).
- , 1987: Small cumuli observed with a 3 mm wavelength Doppler radar. *Geophys. Res. Lett.*, **14**, 707–710, doi:[10.1029/GL014i007p00707](https://doi.org/10.1029/GL014i007p00707).
- Luke, E. P., and P. Kollias, 2013: Separating cloud and drizzle radar moments during precipitation onset using Doppler spectra. *J. Atmos. Oceanic Technol.*, **30**, 1656–1671, doi:[10.1175/JTECH-D-11-00195.1](https://doi.org/10.1175/JTECH-D-11-00195.1).
- , —, K. L. Johnson, and E. E. Clothiaux, 2008: A technique for the automatic detection of insect clutter in cloud radar returns. *J. Atmos. Oceanic Technol.*, **25**, 1498–1513, doi:[10.1175/2007JTECHA953.1](https://doi.org/10.1175/2007JTECHA953.1).
- , —, and M. D. Shupe, 2010: Detection of supercooled liquid in mixed-phase clouds using radar Doppler spectra. *J. Geophys. Res.*, **115**, D19201, doi:[10.1029/2009JD012884](https://doi.org/10.1029/2009JD012884).
- Mather, J. H., and J. W. Voyles, 2013: The ARM Climate Research Facility: A review of structure and capabilities. *Bull. Amer. Meteor. Soc.*, **94**, 377–392, doi:[10.1175/BAMS-D-11-00218.1](https://doi.org/10.1175/BAMS-D-11-00218.1).
- Matrosov, S. Y., G. G. Mace, R. T. Marchand, M. D. Shupe, A. G. Hallar, and I. B. McCubbin, 2012: Observations of ice crystal habits with a scanning polarimetric W-band radar at slant linear depolarization ratio mode. *J. Atmos. Oceanic Technol.*, **29**, 989–1008, doi:[10.1175/JTECH-D-11-00131.1](https://doi.org/10.1175/JTECH-D-11-00131.1).
- McFarquhar, G. M., and Coauthors, 2011: Indirect and Semi-Direct Aerosol Campaign: The impact of Arctic aerosols on clouds. *Bull. Amer. Meteor. Soc.*, **92**, 183–201, doi:[10.1175/2010BAMS2935.1](https://doi.org/10.1175/2010BAMS2935.1).
- Mead, J. B., A. L. Pazmany, S. M. Sekelsky, and R. E. McIntosh, 1994: Millimeter-wave radars for remotely sensing clouds and precipitation. *Proc. IEEE*, **82**, 1891–1905, doi:[10.1109/5.338077](https://doi.org/10.1109/5.338077).
- Miller, M. A., and B. A. Albrecht, 1995: Surface-based observations of mesoscale cumulus–stratocumulus interaction during ASTEX. *J. Atmos. Sci.*, **52**, 2809–2826, doi:[10.1175/1520-0469\(1995\)052<2809:SBOOMC>2.0.CO;2](https://doi.org/10.1175/1520-0469(1995)052<2809:SBOOMC>2.0.CO;2).
- Moran, K. P., B. E. Martner, M. J. Post, R. A. Kropfli, D. C. Welsh, and K. B. Widener, 1998: An unattended cloud-profiling radar for use in climate research. *Bull. Amer. Meteor. Soc.*, **79**, 443–455, doi:[10.1175/1520-0477\(1998\)079<0443:AUCPRF>2.0.CO;2](https://doi.org/10.1175/1520-0477(1998)079<0443:AUCPRF>2.0.CO;2).
- O'Connor, E. J., R. J. Hogan, and A. J. Illingworth, 2005: Retrieving stratocumulus drizzle parameters using Doppler radar and lidar. *J. Appl. Meteor.*, **44**, 14–27, doi:[10.1175/JAM-2181.1](https://doi.org/10.1175/JAM-2181.1).
- Pasqualucci, F., B. W. Bartram, R. A. Kropfli, and W. R. Moninger, 1983: A millimeter-wavelength dual-polarization Doppler radar for cloud and precipitation studies. *J. Climate Appl. Meteor.*, **22**, 758–765, doi:[10.1175/1520-0450\(1983\)022<0758:AMWDPD>2.0.CO;2](https://doi.org/10.1175/1520-0450(1983)022<0758:AMWDPD>2.0.CO;2).
- Platt, C. M. R., J. C. Scott, and A. C. Dilley, 1987: Remote sounding of high clouds. Part IV: Optical properties of midlatitude and tropical cirrus. *J. Atmos. Sci.*, **44**, 729–747, doi:[10.1175/1520-0469\(1987\)044<0729:RSOHCPC>2.0.CO;2](https://doi.org/10.1175/1520-0469(1987)044<0729:RSOHCPC>2.0.CO;2).
- Ramanathan, V., R. D. Cess, E. F. Harrison, P. Minnis, B. R. Barkstrom, E. Ahmad, and D. Hartmann, 1989: Cloud-radiative forcing and climate: Results from the Earth Radiation Budget Experiment. *Science*, **243**, 57–63, doi:[10.1126/science.243.4887.57](https://doi.org/10.1126/science.243.4887.57).
- Sassen, K., C. J. Grund, J. D. Spinhirne, M. H. Hardesty, and J. M. Alvarez, 1990: The 27–28 October FIRE IFO cirrus case study: A five lidar overview of cloud structure and evolution. *Mon. Wea. Rev.*, **118**, 2288–2311, doi:[10.1175/1520-0493\(1990\)118<2288:TOFICC>2.0.CO;2](https://doi.org/10.1175/1520-0493(1990)118<2288:TOFICC>2.0.CO;2).
- , and Coauthors, 1995: The 5–6 December 1991 FIRE IFO II jet stream cirrus case study: Possible influences of volcanic aerosols. *J. Atmos. Sci.*, **52**, 97–123, doi:[10.1175/1520-0469\(1995\)052<0097:TDFIJJ>2.0.CO;2](https://doi.org/10.1175/1520-0469(1995)052<0097:TDFIJJ>2.0.CO;2).
- Shupe, M. D., P. Kollias, S. Y. Matrosov, and T. L. Schneider, 2004: Deriving mixed-phase cloud properties from Doppler radar spectra. *J. Atmos. Oceanic Technol.*, **21**, 660–670, doi:[10.1175/1520-0426\(2004\)021<0660:DMCPFD>2.0.CO;2](https://doi.org/10.1175/1520-0426(2004)021<0660:DMCPFD>2.0.CO;2).
- , and Coauthors, 2008: A focus on mixed-phase clouds: The status of ground-based observational methods. *Bull. Amer. Meteor. Soc.*, **89**, 1549–1562, doi:[10.1175/2008BAMS2378.1](https://doi.org/10.1175/2008BAMS2378.1).
- , J. M. Comstock, D. D. Turner, and G. G. Mace, 2016: Cloud property retrievals in the ARM Program. *The Atmospheric Radiation Measurement (ARM) Program: The First 20 Years*, Meteor. Monogr., No. 57, Amer. Meteor. Soc., doi:[10.1175/AMSMONOGRAPHS-D-15-0030.1](https://doi.org/10.1175/AMSMONOGRAPHS-D-15-0030.1).
- Sisterson, D., R. Peppler, T. S. Cress, P. Lamb, and D. D. Turner, 2016: The ARM Southern Great Plains (SGP) site. *The Atmospheric Radiation Measurement (ARM) Program: The First*

- 20 Years, *Meteor. Monogr.*, No. 57, Amer. Meteor. Soc., doi:[10.1175/AMSMONOGRAPHIS-D-16-0004.1](https://doi.org/10.1175/AMSMONOGRAPHIS-D-16-0004.1).
- Stokes, G. M., 2016: Original ARM concept and launch. *The Atmospheric Radiation Measurement (ARM) Program: The First 20 Years, Meteor. Monogr.*, No. 57, Amer. Meteor. Soc., doi:[10.1175/AMSMONOGRAPHIS-D-15-0021.1](https://doi.org/10.1175/AMSMONOGRAPHIS-D-15-0021.1).
- , and S. E. Schwartz, 1994: The Atmospheric Radiation Measurement (ARM) Program: Programmatic background and design of the cloud and radiation test bed. *Bull. Amer. Meteor. Soc.*, **75**, 1201–1221, doi:[10.1175/1520-0477\(1994\)075<1201:TARMPP>2.0.CO;2](https://doi.org/10.1175/1520-0477(1994)075<1201:TARMPP>2.0.CO;2).
- Tridon, F., A. Battaglia, P. Kollias, E. Luke, and C. R. Williams, 2013: Signal postprocessing and reflectivity calibration of the Atmospheric Radiation Measurement Program 915-MHz wind profilers. *J. Atmos. Oceanic Technol.*, **30**, 1038–1054, doi:[10.1175/JTECH-D-12-00146.1](https://doi.org/10.1175/JTECH-D-12-00146.1).
- Turner, D. D., and Coauthors, 2007: Thin liquid water clouds: Their importance and our challenge. *Bull. Amer. Meteor. Soc.*, **88**, 177–190, doi:[10.1175/BAMS-88-2-177](https://doi.org/10.1175/BAMS-88-2-177).
- Uttal, T., E. E. Clothiaux, T. P. Ackerman, J. M. Intrieri, and W. L. Eberhard, 1995: Cloud boundary statistics during FIRE II. *J. Atmos. Sci.*, **52**, 4276–4284, doi:[10.1175/1520-0469\(1995\)052<4276:CBSDFI>2.0.CO;2](https://doi.org/10.1175/1520-0469(1995)052<4276:CBSDFI>2.0.CO;2).
- Verlinde, J., and Coauthors, 2007: The Mixed-Phase Arctic Cloud Experiment. *Bull. Amer. Meteor. Soc.*, **88**, 205–221, doi:[10.1175/BAMS-88-2-205](https://doi.org/10.1175/BAMS-88-2-205).
- Widener, K. B., A. S. Koontz, K. P. Moran, K. A. Clark, C. Chander, M. A. Miller, and K. L. Johnson, 2004: MMCR upgrades: Present status and future plans. *Proc. 14th Atmospheric Radiation Measurement (ARM) Science Team Meeting*, Albuquerque, NM, U.S. DOE. [Available online at http://www.arm.gov/publications/proceedings/conf14/extended_abs/widener1-kb.pdf.]